International Journal of Biological Macromolecules 122 (2019) 1152–1162

Contents lists available at ScienceDirect

International Journal of Biological Macromolecules

journal homepage: http://www.elsevier.com/locate/ijbiomac

Hydrogels of agarose, and methacrylated gelatin and hyaluronic acid are more supportive for *in vitro* meniscus regeneration than three dimensional printed polycaprolactone scaffolds

Gokhan Bahcecioglu [a,b,c], Nesrin Hasirci [a,c,d], Bahar Bilgen [e,f,g,*], Vasif Hasirci [a,b,c,**,1]

[a] BIOMATEN, Center of Excellence in Biomaterials and Tissue Engineering, Middle East Technical University (METU), Ankara, Turkey
[b] Department of Biological Sciences, METU, Ankara, Turkey
[c] Department of Biotechnology, METU, Ankara, Turkey
[d] Department of Chemistry, METU, Ankara, Turkey
[e] Providence VA Medical Center, Providence, RI, United States of America
[f] Department of Orthopaedics, The Warren Alpert Medical School of Brown University, Providence, RI, United States of America
[g] Rhode Island Hospital, Providence, RI, United States of America

ARTICLE INFO

Article history:
Received 26 June 2018
Received in revised form 10 September 2018
Accepted 11 September 2018
Available online 12 September 2018

Keywords:
Hydrogels
3D printed PCL
Meniscal regeneration

ABSTRACT

In this study, porcine fibrochondrocyte-seeded agarose, methacrylated gelatin (GelMA), methacrylated hyaluronic acid (MeHA) and GelMA-MeHA blend hydrogels, and 3D printed PCL scaffolds were tested under dynamic compression for potential meniscal regeneration *in vitro*. Cell-carrying hydrogels produced higher levels of extracellular matrix (ECM) components after a 35-day incubation than the 3D printed PCL. Cells on GelMA exhibited strong cell adhesion (evidenced with intense paxillin staining) and dendritic cell morphology, and produced an order of magnitude higher level of collagen ($p < 0.05$) than other materials. On the other hand, cells in agarose exhibited low cell adhesion and round cell morphology, and produced higher levels of glycosaminoglycans (GAGs) ($p < 0.05$) than other materials. A low level of ECM production and a high level of cell proliferation were observed on the 3D printed PCL. Dynamic compression at 10% strain enhanced GAG production in agarose ($p < 0.05$), and collagen production in GelMA. These results show that hydrogels have a higher potential for meniscal regeneration than the 3D printed PCL, and depending on the material used, fibrochondrocytes could be directed to proliferate or produce cartilaginous or fibrocartilaginous ECM. Agarose and MeHA could be used for the regeneration of the inner region of meniscus, while GelMA for the outer region.

1. Introduction

Meniscus is a semilunar, fibrocartilaginous tissue in the knee joint that has many functions including load bearing and transmission, shock absorption, and joint lubrication. The outer periphery of the meniscus is fibrous and contains high amounts of type I collagen (COL I) and fibroblast-like cells with long cell processes, while the inner region is cartilaginous and contains high amounts of type II collagen (COL II), glycosaminoglycans (GAGs), and chondrocyte-like cells with round or polygonal morphology [1].

Meniscal tears are among the most widely encountered problems in the knee joint. Tears in the inner region of the meniscus have limited healing capacity, because of the limited vascularity in this region. Attempts to repair meniscal tears include the use of fibrin glue and sutures [2], and rasping [3], which have success rates higher than 70%. However, these methods may lead to fibrous scar formation, which may interfere with the meniscus biomechanics. In case of more serious injuries, partial meniscectomy is performed, but that may lead to osteoarthritis (OS) in the long term [4]. Transplants have the disadvantage of donor scarcity and risks of rejection and disease transmission [5]. In addition, transplantation of meniscal allografts does not prevent or delay osteoarthritis [6]. Tissue engineering appears to be a viable alternative for meniscal replacement and regeneration.

Scaffolds are of utmost importance in tissue engineering applications, because they accommodate the cells and guide them to produce the target tissue, and provide the necessary mechanical strength before the new tissue is formed. Three-dimensional (3D) printing has been in the spotlight of tissue engineering field because of its many advantages

* Correspondence to: B. Bilgen, 1 Hoppin Street, Coro West, Rm: 4.312, Providence, RI 02903, United States of America.
** Correspondence to: V. Hasirci, 1 Dumlupinar Blvd, BIOMATEN Rm: 101, METU, Cankaya, Ankara 06800, Turkey.
E-mail addresses: bahar_bilgen@brown.edu (B. Bilgen), vhasirci@metu.edu.tr (V. Hasirci).
[1] Department of Medical Engineering, Acibadem Mehmet Ali Aydinlar University, Atasehir, Istanbul, Turkey.

https://doi.org/10.1016/j.ijbiomac.2018.09.065
0141-8130/

including production speed, accuracy, reproducibility and reliability [7]. Polycaprolactone (PCL) is one of the most commonly used polymers in melt-based extrusion printing to produce scaffolds, because of its biocompatibility, relatively low melting temperature (60 °C), and good rheological and viscoelastic properties [8,9]. The disadvantage of PCL is the lack of biofunctional groups on its polymer chains, which limits adhesion and guidance of cells to produce the target tissue. Therefore, PCL scaffolds have been blended or coated with hydrophobic [10,11] and hydrophilic [12] polymers to improve cell adhesion and extracellular matrix (ECM) production. Hydrogels of natural polymers could be used to introduce bioactivity to the PCL scaffolds, and enhance cell viability.

Hydrogels, hydrophilic polymer networks that can absorb large amounts of water, are of particular importance in producing tissue engineering scaffolds for cartilaginous tissues, because of their biocompatibility, bioactivity, and structural similarity to the ECM [13,14]. Many hydrogels have been used in the regeneration of cartilaginous tissues, including agarose [15–17], alginate [18,19], collagen [20,21], gelatin [22], hyaluronic acid (HA) [23], and the photoactive polymers methacrylated gelatin (GelMA) and HA (MeHA) [17,24,25]. However, these hydrogels have not been extensively tested for meniscal regeneration.

The aim of this study was to investigate the potentials of hydrogels and 3D printed PCL scaffolds for meniscal regeneration, and selection of the appropriate hydrogels for possible combination with the PCL scaffolds. Porcine fibrochondrocyte-seeded agarose, GelMA, MeHA and GelMA-MeHA hydrogels and PCL scaffolds were tested *in vitro* under dynamic compression for production of COL I, COL II and GAGs. In order to mimic the cyclic load exerted on the menisci during physiological conditions, dynamic compression at 10% strain was applied. Stability, cell viability, ECM production, and cell-material interactions on the scaffolds were studied.

2. Materials and methods

2.1. Tissue and cell harvest

Medial menisci were harvested from two postmortem Yorkshire pigs (female, 3 months old) according to the Lifespan Institutional Animal Care and Use Committee (IACUC) Policy for the Responsible Conduct of Animal Research and Use of Central Research Facilities (USA) which requires no review.

Menisci were minced and digested overnight at 37 °C in type II collagenase (0.15%, w/v). Digests were incubated in growth medium (DMEM-F12 (1:1) and 1% ITS+ Premix (Thermo Fisher Scientific, USA), 10% FBS (Atlanta Biologicals, USA), 100 U/mL penicillin/streptomycin and 1 μg/mL amphotericin B (Thermo Fisher Scientific, USA)) at 37 °C for cell expansion [26]. Fibrochondrocytes were trypsinized at confluence, frozen and stored at −80 °C until use.

2.2. Preparation of the constructs

2.2.1. Preparation of PCL scaffolds

Poly (ε-caprolactone) (Sigma-Aldrich, USA) (Mw:50 kDa) was loaded into cartridges of Bioscaffolder system (SYS + ENG, Salzgitter-Bad, Germany), melt at 150 °C, and 3D printed in square prism shapes (4 mm × 4 mm × 3 mm), and with 0–90° strand orientation and 1 mm strand distance. PCL samples were sterilized with ethanol before use.

Fibrochondrocytes were suspended in growth medium and seeded on PCL at a final density of 2×10^5 cells/scaffold.

2.2.2. Methacrylation of gelatin and hyaluronic acid

Gelatin (from bovine skin, 225 Bloom) solution (10% *w/v*, in PBS, pH 7.2) and methacrylic anhydride (MA) (Sigma-Aldrich, USA) were mixed (Gelatin:MA, 7:1, *v*/v) and incubated at 50 °C for 1.5 h to obtain GelMA [27,28]. Hyaluronic acid (HA, from *Streptococcus equi*, Sigma-Aldrich) (M_w: 0.6–1.1 MDa) solution (0.5% w/v, in distilled water: dimethylformamide (3:2, v/v)) and MA were mixed (HA:MA, 99:1, v/v) and incubated overnight at 4 °C to obtain MeHA [29]. The solutions were dialyzed against phosphate buffer (pH 7.2) for 3 days, frozen at −80 °C and lyophilized. The resulting polymers were sterilized with ethylene oxide and stored at −20 °C until use.

Gelatin and GelMA (50 mg/mL), and MeHA (1 mg/mL) were dissolved in deuterium oxide at 35 °C and the solutions were characterized with Proton (^{1}H) NMR spectrometer (Bruker DPX 400) operating at a ^{1}H resonance frequency of 400 MHz. The degrees of methacrylation (DM) were calculated as described previously [30,31]. Briefly DM of GelMA was calculated from the peak integration (area) of the protons of the lysyl methylene groups (peak at 2.90 ppm) in unmodified gelatin relative to that in GelMA using the NMR spectrum analysis software (MestreNova, Spain) (Fig. S1a). The peak integrations were normalized to the phenylalanine (the aromatic group which does not exhibit any shift in the intensity of NMR spectrum) (peak at 7.2 ppm) to eliminate the concentration differences. DM of MeHA was calculated from the ratio of the peak integrations of the protons of the methacrylate groups in MeHA (peak at 1.85 ppm) to methyl protons (peak at 1.9 ppm) (Fig. S1b).

2.2.3. Construction of cell-laden hydrogels

Agarose (type VII, low gelling temperature) (Sigma-Aldrich) solution (2%, *w/v*, in DMEM:F12 (1:1)) was sterilized using a microwave and cooled down to 43 °C before adding cells. GelMA (6.4%, *w/v*), MeHA (0.8%, w/v), and GelMA-MeHA (3.2% GelMA and 0.4% MeHA) solutions containing 1% (*w/v*) of the photoinitiator (Irgacure D-2959, Sigma-Aldrich) were prepared in growth media. Fibrochondrocytes (passage 2) were reconstituted in the polymer solutions and placed between two glass plates separated by 1.5 mm-thick spacers (Fig. 1a). For gelation, the agarose-cell suspension was cooled, and the photoactive polymer-cell suspensions were exposed to UV (λ: 365 nm) for 5 min. Disks of gels (diameter: 5 mm, thickness: 1.5 mm) (Fig. 1a) with cell densities of around 2×10^5 cells/sample were obtained.

2.3. Cell culture and mechanical stimulation

Constructs were incubated in growth medium at 37 °C for 7 days, followed by 28 days in fibrochondrogenic medium (growth medium containing 40 mM L-proline, 1 mM nonessential amino acids NEAA, and 50 μg/mL L-ascorbic acid 2-phosphate) (Fig. 1b). Dexamethasone (Sigma-Aldrich) (100 nM), and TGF-β1 (R&D Systems, USA) (10 ng/mL) were added on alternate days at every medium change between Days 7–28. Constructs were incubated under static (no load) or dynamic culture conditions between Days 7–35. Dynamic compression at 10% strain (superimposed on a 5% static strain) was performed 1 h/day, 5 days/week, and at 1 Hz frequency in a custom-made bioreactor with a polysulfone platen that fits in 24-well culture plates [32] (Fig. 1c).

2.4. Mechanical testing

Samples ($n = 5$–6) were removed from culture on Day 35 and subjected to mechanical testing using Instron (ElectroPuls, E1000, USA) with 10 N-load cell. A stress-relaxation test was performed; unconfined compression at 10% strain based on sample thickness was maintained for a 30 min of relaxation period until equilibrium. The equilibrium modulus was calculated using the stress at equilibrium.

2.5. Contraction and weight loss of the constructs

Samples were examined macroscopically every week during the culture period. Thickness and diameter of the samples were measured on Days 1 and 35 using a micrometer, and the volume calculated. Samples

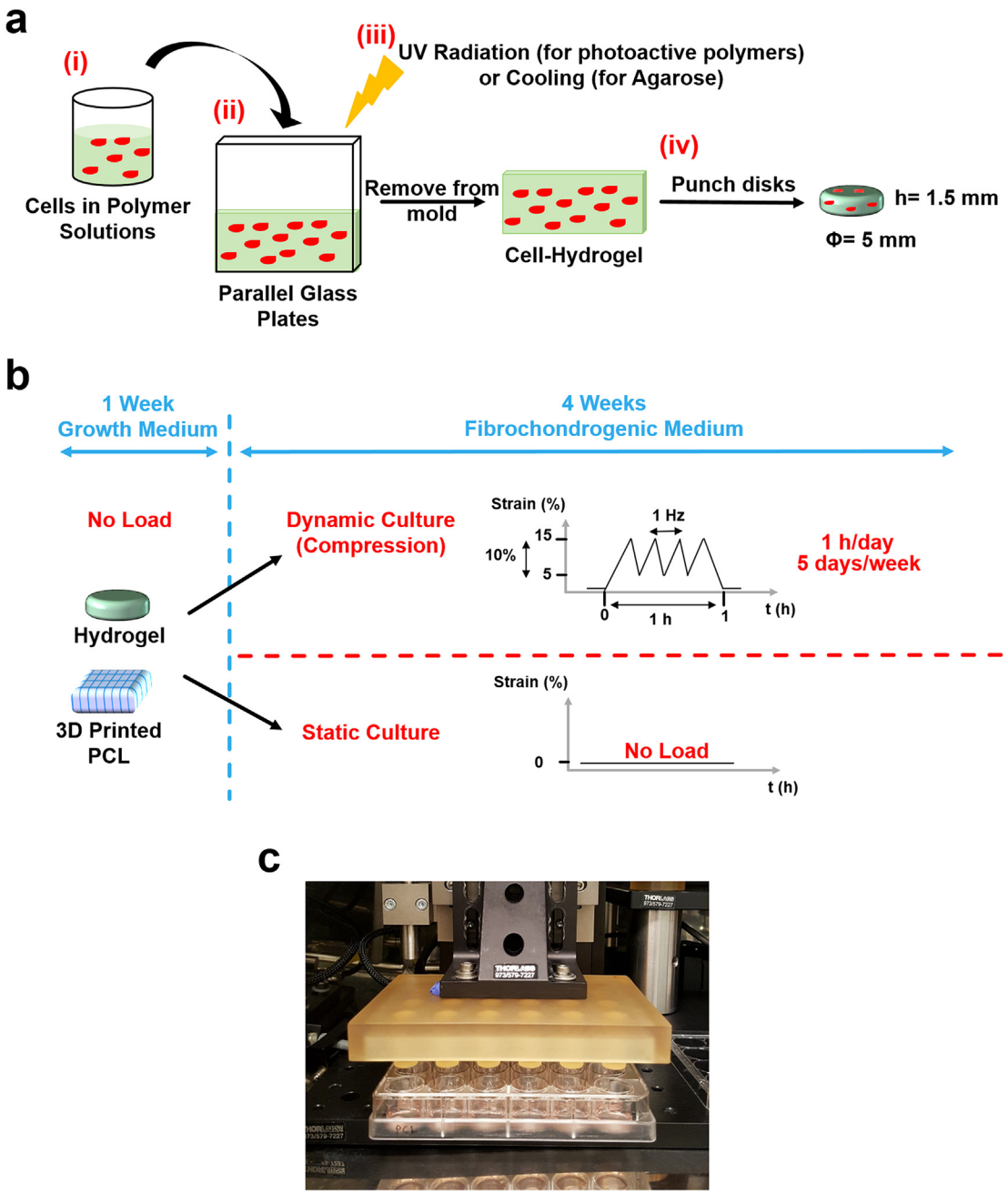

Fig. 1. Scaffold preparation and culture conditions. (a) Preparation of the hydrogels. (i) Cell suspensions were prepared in agarose, GelMA, MeHA, and GelMA-MeHA solutions. (ii) Cell-polymer suspensions were cast between two parallel plates separated with a spacer. (iii) Agarose was cooled and other polymers were UV irradiated for gelation to take place. (iv) Disks of gels were obtained using a tissue punch. (b) Culture conditions. Constructs were incubated for 1 week in growth medium, followed by 4 weeks in fibrochondrogenic medium under static or dynamic conditions. Starting on Day 7, dynamic compression at 10% strain was applied for 4 weeks at 1 Hz frequency, 1 h/day, 5 days/week in a (c) custom-made bioreactor.

were weighed (wet weight, WW), frozen at −20 °C, lyophilized for 24 h, and weighed again (dry weight, DW).

2.6. Biochemical assays

Lyophilized samples ($n = 3$–6) were digested overnight at 60 °C in papain solution (125 U/mL) (Sigma-Aldrich). DNA, sulfated glycosaminoglycan (sGAG), and collagen contents of the samples were determined using PicoGreen® (Life Technologies, USA), 1,9-dimethylmethylene blue (pH 3.0), and hydroxyproline assays, respectively. Collagen content was determined using a hydroxyproline to collagen weight ratio of 1:7.64 [33]. Relative DNA content was the DNA content of a sample on Day 35 relative to that on Day 1. GAG and collagen contents were normalized to the DWs of the samples. Meniscus tissue was used as a positive control.

2.7. Cell viability

Cell viability was assessed using Live/Dead™ cell viability/cytotoxicity kit (Thermo Fisher Scientific). Samples were removed from culture on Day 35, incubated in a solution containing Calcein-AM (2 μM in PBS) and ethidium homodimer (EthD)-1 (4 μM) for 30 min and visualized using a confocal laser scanning microscope (CLSM) (Nikon C1Si, Japan). Semi-quantitative image analysis ($n \geq 2$) was

performed using ImageJ (NIH, USA) to assess cell viability by calculating the percentage of live cells (green) in a sample (total cells: green and red). Constructs were also imaged using phase contrast microscopy.

Cell metabolic activity was monitored during the culture period using alamarBlue® assay (Thermo Fisher Scientific). Samples ($n \geq 10$) were washed in PBS and incubated in alamarBlue solution (10% *v*/v in colorless growth medium) for 1 h. Absorbance of the supernatants were determined at 570 nm and 595 nm, and percent reduction of the dye (correlated with cell metabolic activity) was calculated according to the manufacturer's instructions.

2.8. Immunohistochemistry and histology

On Day 35, hydrogels ($n = 3$ for seeded, and $n = 1$ for unseeded) were fixed in acetone/methanol (1:1, *v*/v), embedded in paraffin and sectioned (6 μm thick). For immunohistochemistry, sections were deparaffinized, treated with pepsin (Thermo Fisher Scientific), and incubated in mouse primary antibodies against COL I (Sigma-Aldrich, Cat. No: C2456) (dilution, 1:100) or COL II (Thermo Fisher Scientific, Cat. No: MS235P1) (dilution, 1:100). Sections were treated with biotinylated horse anti-mouse IgG, avidin-biotin complex (Vectastain ABC kit, Vector Laboratories, USA) (Cat. No: PK-4002), and 3,3-diaminobenzidine (DAB) chromogen (Horse radish peroxidase kit, Vector Laboratories, USA). Sections were counterstained with hematoxylin and imaged using a bright-field microscope. Semi-quantitative image analysis was performed to assess the intensity of staining (ImageJ). Briefly, micrographs were converted to 8-bit images, and the integrated density calculated after background subtraction. For each construct, 2–9 images per sample were used.

For histology, sections were stained with Safranin-O (for GAGs), and counterstained with Fast Green (for cells and proteins). Meniscus and hyaline cartilage were used as positive controls.

2.9. Cell-material interactions and cell morphology on hydrogels

In order to analyze cell-material interactions, hydrogels were stained for paxillin. Cell-seeded samples (Day 21) ($n = 2$) were incubated in 0.1% Triton X-100 at ambient temperature for 5 min, and then in 1% BSA for 30 min, Alexafluor 532-labelled phalloidin (Thermo Fisher Scientific) (to stain F-actin) for 1 h, mouse primary antibody against paxillin (Sigma, Cat. No: P1093) (dilution: 1:100) for 1 h, Alexafluor 488-labelled goat anti-mouse IgG secondary antibody (Thermo Fisher Scientific, Cat. No: A-11001) (dilution 1:400) for 1 h, and DRAQ5 (Cell Signaling Technology, USA) (to stain the nuclei) for 30 min all at 37 °C. Cover slips were used as positive controls. Samples were visualized using CLSM (Leica TCS SPE, Germany).

For examination of gel microarchitecture and cell morphology, cell-free and cell-seeded samples (Day 21) were washed with cacodylate buffer, incubated in glutaraldehyde solution (2.5% in cacodylate buffer), frozen at −80 °C, lyophilized for 3 h, sputter-coated with gold-palladium, and visualized using scanning electron microscope (SEM) (FEI, Quanta 400 F, USA) under high vacuum.

2.10. Statistical analyses

Statistical analyses were performed using SPSS 23 (IBM, USA). Student's *t*-test was performed for comparison of two groups, and one-, two- and three-way ANOVA were performed for comparison of multiple groups depending on the number of independent variables (material, cell seeding, mechanical loading, and time). Levene's test of inequality was performed to test whether samples had equal variance. Tukey's HSD (equal variance) or Dunnett's T3 (unequal variance) *post hoc* tests were applied after ANOVA. A significance level (α) of 0.05 was used. Data are presented as the mean ± standard deviation (SD).

3. Results

3.1. Physical properties of the constructs

Proton NMR revealed that the methacrylation degrees of GelMA (Fig. S1a) and MeHA (Fig. S1b) were 52 and 25%, respectively, similar to those reported previously in our group [30,31].

Macroscopic evaluation revealed significant shrinkage of the cell-seeded GelMA-MeHA over time (Fig. 2a). Quantitative analysis revealed no change in thickness, diameter, volume and dry weight (DW) of the unseeded gels after 35 days of incubation, except for the decrease in DWs of the GelMA-containing gels (Fig. S2). Presence of cells led to significant decreases in the physical properties of all gels ($p < 0.05$), except for agarose and GelMA which increased in thickness and DWs after introduction of cells (compared to unseeded constructs).

3.2. Compressive mechanical properties

After 35 days of incubation in culture media, equilibrium modulus of the 3D printed PCL (unseeded constructs: 2.4 ± 1.2 MPa, and seeded: 4.6 ± 1.8 MPa) was 2–3 orders of magnitude higher ($p < 0.0005$) than those of the hydrogels (for agarose, unseeded constructs: 13.1 ± 1.4 kPa, and seeded: 16.1 ± 1.1 kPa; for GelMA, unseeded constructs: 6.6 ± 1.8 kPa, and seeded: 9.1 ± 2.0 kPa; for MeHA, unseeded constructs: 11.6 ± 1.6 kPa, and seeded: 3.1 ± 0.9 kPa, and for GelMA-MeHA, unseeded constructs: 11.3 ± 2.1 kPa, and seeded: could not be detected). Among the hydrogels, the highest equilibrium modulus was observed with agarose regardless of cell presence ($p < 0.0005$). Introduction of cells increased the modulus of PCL ($p < 0.01$) and GelMA ($p = 0.06$), and decreased those of agarose ($p < 0.05$), MeHA ($p < 0.0005$), and GelMA-MeHA. Dynamic compression had no effect on equilibrium modulus.

3.3. Scaffold microarchitecture

SEM examination revealed that agarose and MeHA were nonporous, and GelMA-containing gels and PCL were porous (Fig. 2b). Pore sizes of GelMA, GelMA-MeHA, and PCL were around 50, 30, and 700 μm, respectively (Fig. 2b, insets).

3.4. DNA contents and cell viability

Relative DNA content, which showed DNA content on Day 35 relative to that on Day 1, was higher on PCL than the hydrogels ($p < 0.0005$) (Fig. 2c). DNA contents of the hydrogels decreased significantly over time, and that of PCL increased. Among all the hydrogels, GelMA (static samples) exhibited the highest DNA content, and GelMA-MeHA exhibited the lowest content. Dynamic compression influenced the DNA content depending on the material used; DNA content of agarose increased significantly upon dynamic compression ($p < 0.05$), while that of GelMA decreased ($p < 0.01$).

Live/dead assay revealed high viability on agarose, GelMA, and PCL, and low viability on MeHA-containing gels (Fig. 2d). ImageJ analysis revealed around 80% cell viability on agarose, GelMA, and PCL, and around 60% viability on MeHA-containing gels. Dynamic compression had no effect on cell viability. Cells were round in agarose and MeHA, dendritic on GelMA, and elongated on PCL (Fig. 2d).

Cell metabolic activity (presented as the reduction of alamarBlue dye) increased until Day 14, and then decreased in all the constructs except for agarose (Fig. S3).

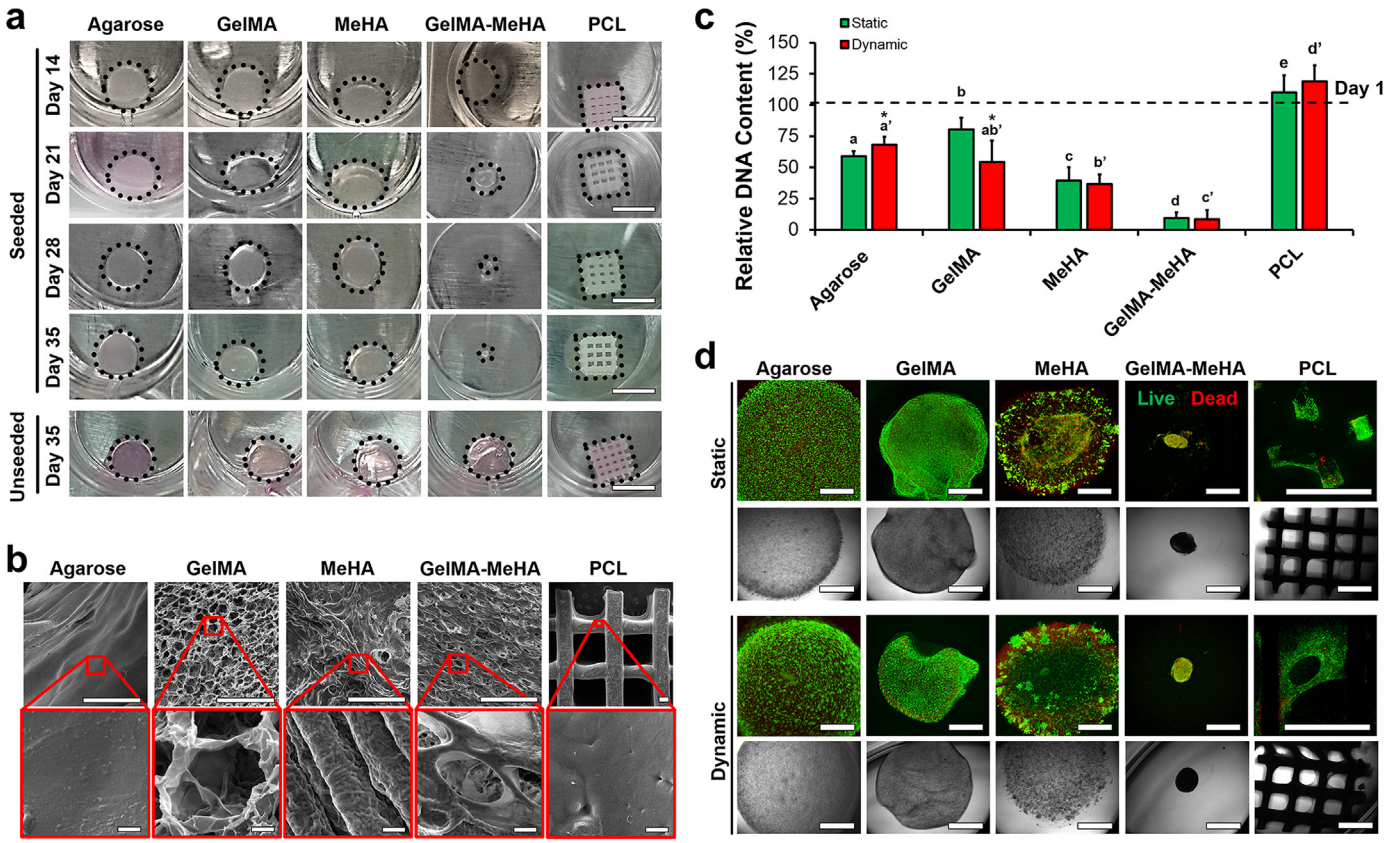

Fig. 2. Macro and microarchitecture of the constructs and cell viability on them. (a) Change in shapes of the constructs over 35 days of culture. Dashed circles and squares mark the construct boundaries. Scale bars: 5 mm. (b) Microarchitecture of the cell-free constructs after 35 days of culture. Scale bars: 200 μm, insets: 10 μm. (c) Relative DNA contents (%): DNA content on Day 35 ($n = 3$–6) relative to Day 1 ($n = 3$, dashed line). Two-way ANOVA showed the effect of dynamic compression depended on the material used. (d) Live/dead assay results on Day 35. CLSM (color) and PC microscopy (black and white) images. Green: calcein-AM (live cells); red: ethidium homodimer-1 (dead cells). Scale bars: 1 mm. [a, b, c, d, e]Significant difference between constructs in the same graph when no letters in common. Comparison within [a, b, c, d, e]static and [a', b', c', d']dynamic groups. *Significant difference between static and dynamic groups of a particular material.

GelMA-MeHA gels degraded almost completely in 35 days, and thus were excluded from the following tests.

3.5. Biochemical assays

3.5.1. Collagen content

The highest collagen content was observed on GelMA (Fig. 3a). Collagen content of GelMA increased significantly over time, and the net increase was 14–18% of the sample DW (Fig. 3a, top). On the other hand, collagen contents of agarose, MeHA, and PCL did not change over time (net change <0.3% of DW). Dynamic compression had no significant effect on collagen production, although collagen content of GelMA increased slightly upon dynamic compression ($p > 0.05$). Collagen contents of the inner and outer regions of the meniscus were 85 and 96% of their DWs, respectively (Fig. 3b, left).

3.5.2. Sulfated glycosaminoglycan (sGAG) contents

Sulfated GAG contents of the hydrogels were higher than that of PCL, with the highest sGAG content being in agarose (Fig. 3a). sGAG content of agarose increased significantly after 35 days of culture ($p < 0.001$), and dynamic compression further increased the sGAG content ($p < 0.05$ compared to static group) (Fig. 3a, bottom). sGAG contents of GelMA ($p < 0.01$) and MeHA ($p > 0.05$) increased over time, but that of PCL did not change. Net sGAG production after 35 days of culture period was the highest on agarose (0.7% sGAG/DW) ($p < 0.01$ compared other hydrogels), which was lower than the results for the native meniscus (1.1% of the DW in the outer region and 2.1% in the inner region) (Fig. 3b, right).

3.6. Immunohistochemistry and histology

Immunohistochemistry revealed the highest deposition of COL I and COL II on GelMA gels (Fig. 4a). Collagen deposition was low on agarose and MeHA. Cross and horizontal sections exhibited intense staining throughout the gels, although GelMA exhibited more intense staining on the surface than the center of the gels. Intense COL I and COL II staining was observed on the native meniscus.

Semi-quantitative analysis revealed that the most intense COL I (25 A.U) ($p < 0.001$) and COL II staining (10 A.U) ($p < 0.05$) were on GelMA (Fig. 4b). A little background COL I (7 A.U) and COL II (3 A.U) staining was observed on the unseeded samples. The net COL I and COL II intensities corrected for the background were 18 and 7 A.U, respectively, which were higher than agarose and MeHA ($p < 0.05$) and lower ($p < 0.05$) than the native meniscus (around 40 A.U for COL I and COL II in the inner region of the meniscus, and 55 A.U for COL I and 30 A.U for COL II in the outer region). Agarose and MeHA exhibited significantly lower COL I ($p < 0.01$) and COL II ($p < 0.05$) staining (net 1–2 A.U) than GelMA.

The ratio of COL II to COL I in agarose and MeHA was around 1, a value close to that of the inner region of the native meniscus (Fig. 4b). In GelMA, it was around 0.5 – a value close to that of the outer region of the meniscus.

3.7. Regional differences in collagen content of the hydrogels

Collagen deposition was higher on the surface (S) of GelMA than in the center (C) (Fig. 5a and b), and semi-quantitative analysis using ImageJ revealed that this difference was significant (higher intensity

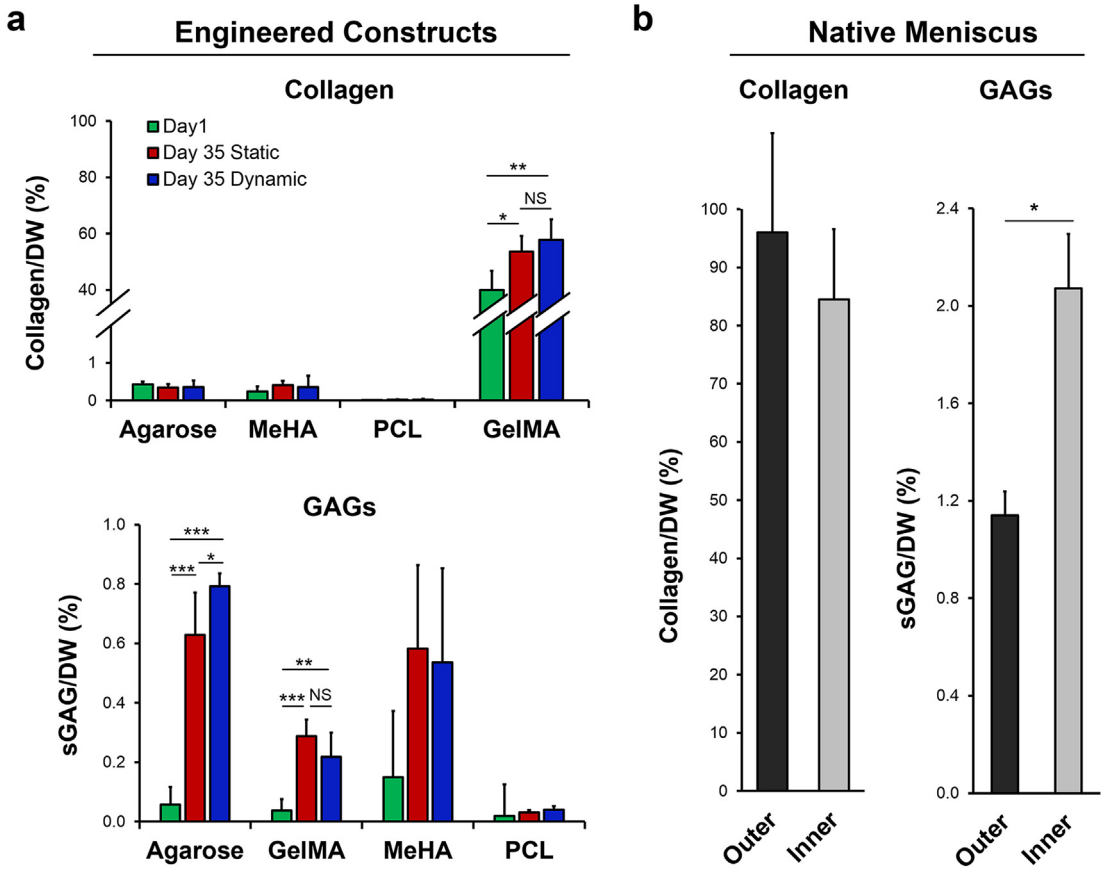

Fig. 3. Collagen and glycosaminoglycan (GAG) contents of the constructs and native meniscus as determined with OHP assay. (a) Collagen (top) and sulfated GAG (bottom) contents of the engineered constructs on Days 1 ($n = 3$) and 35 ($n = 6$). One-way ANOVA was performed to compare Day 1, Day 35 Static (no load), and Day 35 Dynamic (compressive load) results for each material, followed by Tukey's HSD *post hoc*. (b) Collagen (left) and sulfated GAG (right) contents of the native meniscus ($n = 6$). Student's *t*-test was performed to compare collagen contents of the outer and inner regions of the meniscus. Data are presented as the mean ± SD. Statistical significance: $^{*}p < 0.05$, $^{**}p < 0.01$, $^{***}p < 0.001$. NS: not significant.

of COL I ($p < 0.001$) and COL II ($p < 0.001$) on the surface of GelMA than in the center). High collagen production was observed in MeHA gels at points where cells were aggregated (Fig. 5a and b).

3.8. Cell morphology

Cells were mainly round in agarose, and they formed aggregates on the surface (Fig. 5c). Most of the cells in the center of GelMA were round with presence of some dendritic cells, and most of the cells on the surface were dendritic. Cells in MeHA were round at sites where they were embedded in the gel and dendritic in the large pores. Cells in the inner region of the native meniscus were mainly round, while those in the outer region were mainly dendritic and/or elongated.

SEM (Fig. 5d) and CLSM (Fig. 6) both confirmed that cells in agarose and MeHA were round and aggregated, and those in GelMA were mainly dendritic. Cells on the cover glass, which was used as the positive control, were also dendritic.

3.9. Cell adhesion

Cell adhesion was strong on GelMA, and weak on agarose and MeHA (Fig. 6). The most intense paxillin staining, indicating strong cell adhesion, was observed on GelMA, regardless of whether the cells were round (arrowheads) or dendritic (Fig. 6a, left), and cells on GelMA were spread with clear stress fibers (Fig. 6a, right). Quantitative analysis showed that paxillin staining intensity on GelMA was significantly higher than that on Ag or MeHA ($p < 0.05$) (Fig. 6b). Strong paxillin was observed on the cover glass, which was used as a control.

4. Discussion

In this study, we have investigated the potential of fibrochondrocyte-seeded agarose, GelMA, MeHA and GelMA-MeHA hydrogels and 3D printed PCL scaffolds to produce meniscal tissue, and shown that hydrogels support production of meniscal ECM more than PCL. On the other hand, PCL was mechanically stronger and induced cell proliferation (Fig. 2). GelMA and agarose kept cells more viable than other hydrogels (Fig. 2); GelMA induced production of type I and II collagens (Figs. 3 and 4), while agarose and MeHA induced production of GAGs (Fig. 3). GelMA could be used in regeneration of the outer portion of the meniscus, while agarose and MeHA could be used to regenerate the inner portions.

Relative DNA content (Fig. 2c) and cell metabolic activity (Fig. S3) were higher on PCL than the hydrogels, indicating a higher proliferation rate on PCL. This was probably due to the large pores on PCL that allowed oxygen and nutrient transport and stiffness of PCL, both inducing cell proliferation. Hydrogels, on the other hand, limited the proliferation of the cells by entrapping them. GelMA, agarose, and PCL exhibited higher cell viability than MeHA-containing gels (Fig. 2d). The high cell viability in GelMA was probably due to biologic recognition sites on gelatin, including arginine-glycine-aspartic acid (RGD) sequences [34] that could induce cell adhesion (Fig. 6) and proliferation. Cells on the surface of agarose formed spheroid-like aggregates by adhering to each other (Fig. 6), which served as substrates for cell attachment and proliferation. The reason for the low DNA content and cell viability in MeHA could be its high hydrophilicity [35], which again limited cell adhesion (Fig. 6). DNA contents of hydrogels decreased over time (Fig. 2c) probably because of cell and material loss due to degradation (Fig. S2), cell death

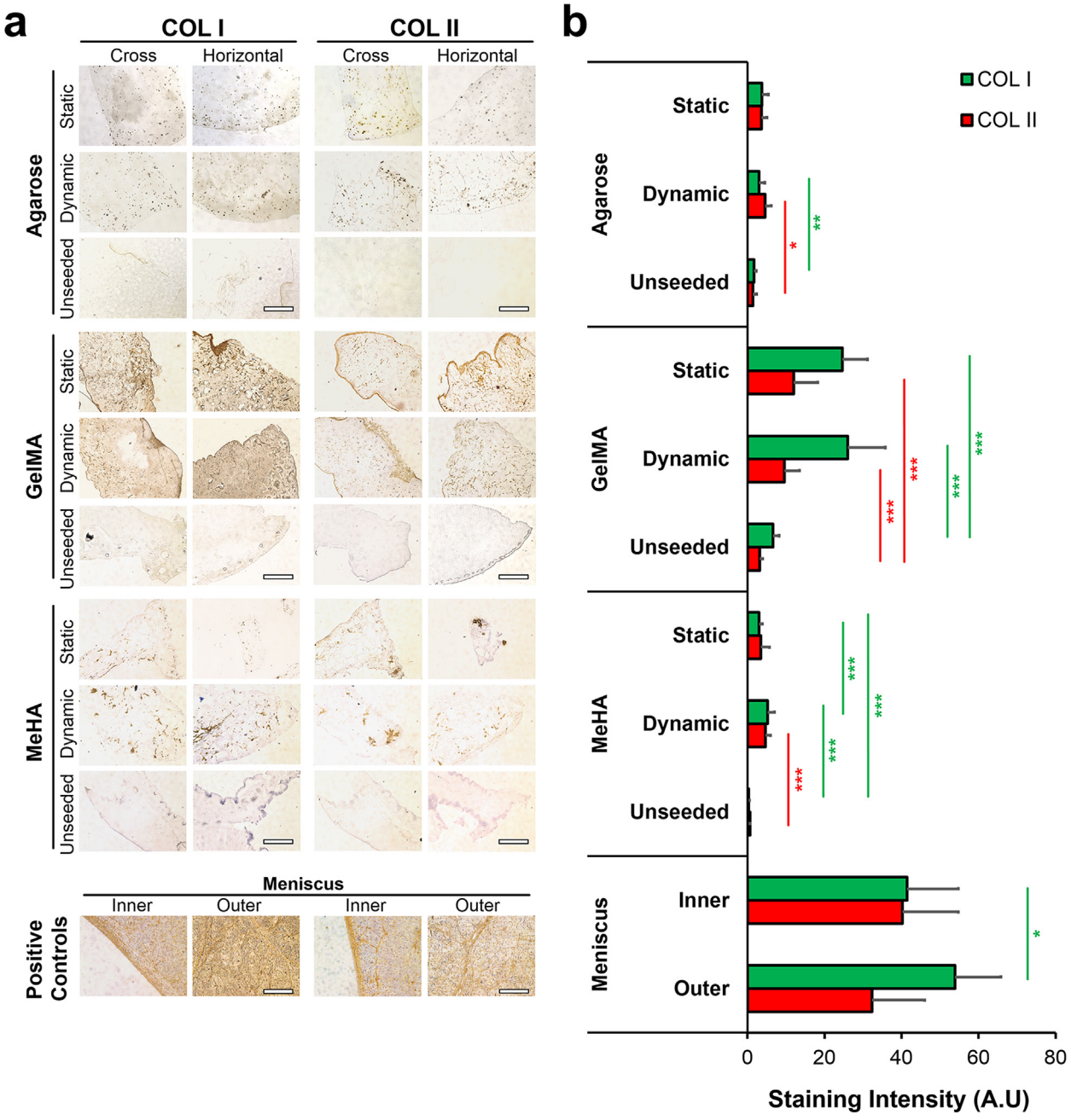

Fig. 4. Immunohistochemistry showing collagen staining on constructs and native meniscus. (a) Immunohistochemistry of the hydrogels stained for COL I and COL II. Positive control: native meniscus. Chromogen: DAB (brown), and counterstain: hematoxylin (dark blue). For the gels, left: cross sections, and right: horizontal sections. Culture time: 35 days. For the native meniscus, left: inner region, and right: outer region. Scale bars: 500 μm. (b) Intensity of COL I and COL II staining (n = 3 samples) measured with ImageJ software (n = 2–9 images/sample). A.U: arbitrary units. *p < 0.05, **p < 0.01, ***p < 0.001. Comparison for COL I (green) or COL II (red) results of a particular material.

(Fig. 2d), and/or decreased rate of cell metabolic activity (cell proliferation) after Day 14 (Fig. S3). Cell metabolic activity peaked at around Day 14 and then decreased, probably because gels started to degrade and lose some material and cells, and/or probably because cells tended to produce ECM after that time rather than proliferate [18].

Fibrochondrocytes in hydrogels were tested for the production of meniscal ECM components – COL I, COL II, and sGAGs. Cells produced the highest amount of collagen in GelMA (COL I and II), and GelMA was the only gel in which collagen content increased significantly over time (Figs. 3 and 4). When cultured under dynamic compression, the net collagen production in GelMA was around 18% of its DW (equivalent to 1.8% of its WW or 235 μg collagen/μg DNA) – about 20–25% of the collagen in the native meniscus obtained in this (85% of its DW in the inner region and 96% in the outer region) (Fig. 3b) and other studies (82% of

Fig. 5. Regional differences in collagen production and cell morphologies in the hydrogels. Representative images of hydrogels (top) stained for (a) COL I, and (b) COL II, and the intensity of staining (bottom) measured with ImageJ software. Chromogen: DAB (brown), and counterstain: hematoxylin (dark blue). Culture time: 35 days. (c) Representative images showing the cell morphologies. Stain: Safranin-O (red), counterstain: Fast Green (green). Insets: high magnifications. Culture time: 35 days. (d) SEM images of the cells on the surface of hydrogels. Culture time: 21 days. C: center; S: surface. A.U: arbitrary units. Scale bars for (a, b, c): 200 μm, and for (d): 20 μm. *Significant difference between intensities in the center and on the surface of a particular gel material at a particular loading regimen.

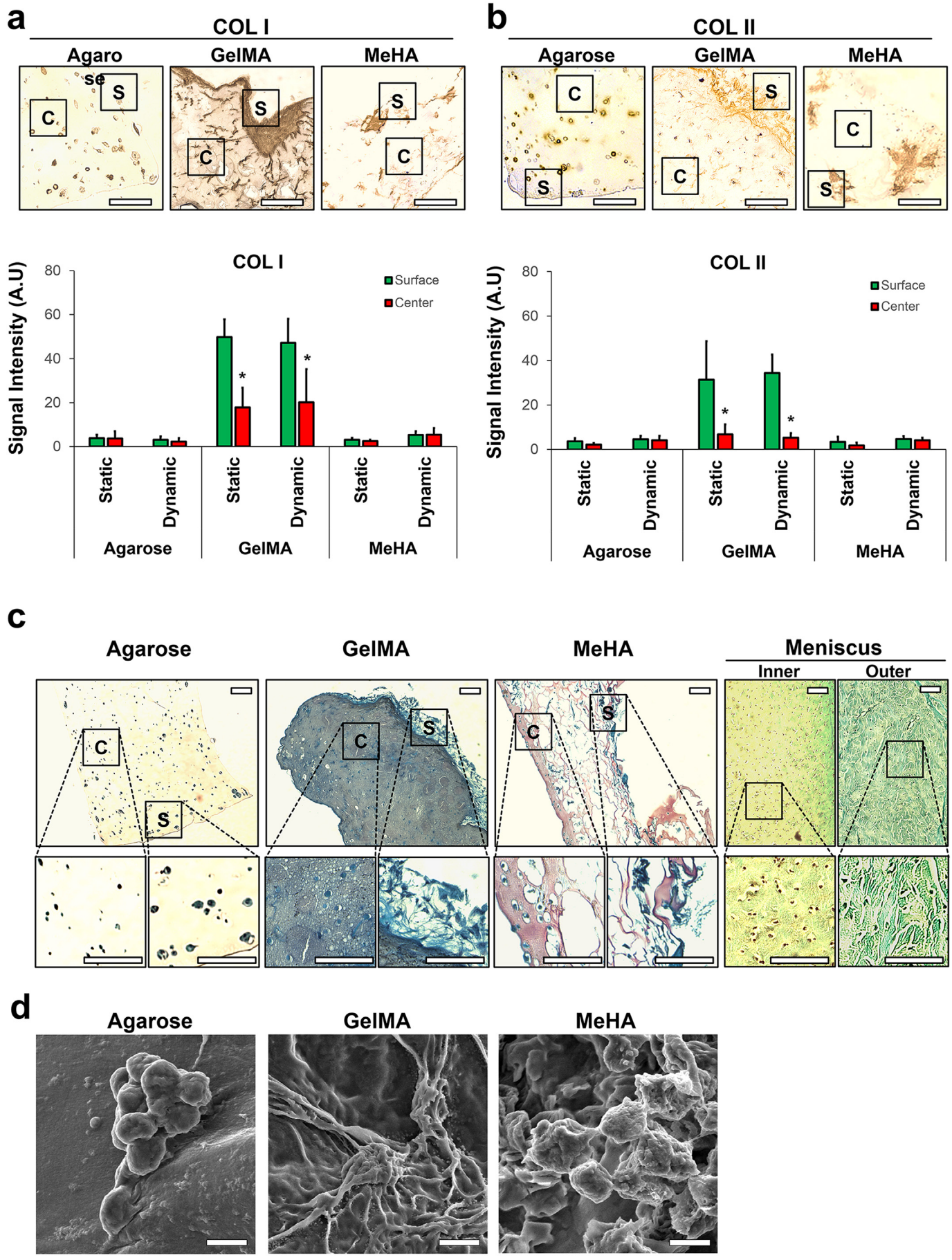
a
COL I
Agaro
se
GelMA
MeHA
S
C
b
COL II
Agarose
GelMA
MeHA
COL I
Signal Intensity (A.U)
Surface
Center
Static
Dynamic
Agarose
GelMA
MeHA
COL II
c
Agarose
GelMA
MeHA
Meniscus
Inner
Outer
d
Agarose
GelMA
MeHA

its DW in the inner region and 90% in the outer region) [1]. Our results were higher than those reported by others employing fibrochondrocyte-seeded collagen gels and reporting 2 μg collagen/μg DNA [20], or 10–20% of the native meniscus [21]. Agarose, MeHA, and PCL all exhibited low amounts of collagen in our study (Figs. 3 and 4). However, the ratio of COL II to COL I was lower in GelMA than in agarose and MeHA (Fig. 4b). Low collagen production was also reported in other studies employing fibrochondrocyte-seeded agarose [16] and PCL [8]. Agarose was also reported to exhibit a higher COL II ratio than GelMA [17]. Our findings are in line with those reported in the literature.

The highest level of GAGs was observed in agarose gels (Fig. 3). The net GAG produced in agarose was 0.74% of its DW (equivalent to 12 μg GAG/μg DNA) (Fig. 3a), about 35–70% of the GAG content of native tissue obtained in this (1–2% of its DW) (Fig. 3b) and other studies (1–4% of its DW) [1]. The net GAG produced in GelMA in this study (0.25% of DW) was lower than that produced in agarose. Similar to our findings, others also reported a higher GAG production in agarose hydrogels than in GelMA [17]. Still others reported decreased expression of aggrecan in fibrochondrocyte-seeded GelMA compared to monolayer expanded cells [24], which indicates that GelMA reduces GAG production.

The different levels and compositions of ECM produced in different hydrogels could be resulted from cell morphology, cell-material interactions and scaffold rigidity, which all could be related. Cells were mainly dendritic/elongated on GelMA and produced high levels of collagen, and mainly round in agarose and MeHA and produced high levels of GAGs (Figs. 3–5). In addition, cells on the surface of GelMA, where they were mainly elongated, produced more COL I and COL II than in the center, where they were mainly round (Fig. 5). Although cells on the surface could proliferate faster and exhibit more ECM because they have better access to nutrients and oxygen, cell morphology still has a considerable effect on ECM production. In fact, collagen production was significantly higher on the surface than in the center of GelMA, but not other hydrogels (Fig. 5a and b). Similar to our findings, fibrochondrocytes in the inner region of the native meniscus are round and produce more GAGs and COL II, while cells in the outer region are dendritic/elongated and produce more COL I [1]. Round cell morphology was also reported to enhance production of cartilaginous ECM components (aggrecan, GAGs and COL II) in collagen and GelMA gels [20,36]. These findings indicate that cell morphology influences ECM production.

Cells in the center of agarose, MeHA, and GelMA were embedded, which might hamper the mobility and spreading of the cells in the center and result in round cell morphology [37,38]. In fact, chondrocytes were reported to maintain their round morphology in agarose gels even after modification with RGD or arginine-glycine-glutamic acid (RGE) sequences [39], and cells embedded in soft agarose gels tended to spread significantly more than the cells in rigid gels [40]. These indicate that the round cell morphology in the center of gels could be a result of their rigid mesh structure. On the other hand, cells were mainly dendritic or elongated on the surface of GelMA, while round on the surface of agarose and MeHA. This shows that the dendritic cell morphology on the surface GelMA is a result of high levels of cell-material interactions (Fig. 6), rather than stiffness.

Cell-material interactions influence the levels and compositions of ECM produced by cells. Collagen production was higher in the center of GelMA than in the centers of agarose or MeHA hydrogels (Fig. 5a and b), although all the cells in these regions were mainly round (Fig. 5c). Cells adhered strongly on GelMA (intense paxillin staining) regardless of the cell morphology (Fig. 6), due to the biologic recognition sites on gelatin [34]. Cells adhered weakly on agarose and MeHA (mild paxillin staining) probably due to high hydrophilicity of these gels [35], and the lack of bioactive sites on these gels that enable cell adhesion. PCL led to elongated cell morphology because it is rigid; however, it lacks bioactive sites, which explains the low ECM production on this scaffold. This indicates that ECM production depends on the material used and is significantly influenced by the cell-material interactions. In parallel with our findings, inhibition of FAKs in GelMA, which hampered cell adhesion, was reported to lead to round cell morphology and induce chondrogenic ECM production [36].

The native meniscus is subject to average compressive strain of up to 12% (ranging between 5 and 15%) under physiologically relevant loading conditions [41]. Therefore, we chose a dynamic compression at 10% strain (oscillating between 5 and 15%) to mimic the physiological strain levels. Dynamic compression in this range led to slightly enhanced production of collagen in GelMA and sGAG in agarose, and to reduced DNA content in GelMA (Figs. 2 and 3). Others have also reported increased collagen and GAG production upon dynamic compression at 10% [42,43] and 15% strain [19]. However, extending the duration of dynamic compression from 2 to 4 weeks, was reported to decrease the ECM production to the initial levels, which explains the slight increases in our study upon dynamic stimulation of the constructs. Moreover, the increase in thickness of agarose and GelMA over time resulted in increased magnitude of the maximal strain from 15% target strain to 18% and 22% actual strain, respectively, which were high and could result in negative effects on ECM production. In fact, dynamic compression at 20% strain leads to reduced production of ECM [44]. These results show that GelMA and agarose could endure compressive strain at physiological levels (5–15% strain) if implanted in the knee.

Equilibrium moduli of the constructs were calculated after 35 days of culture period. Modulus of PCL (2.3 MPa) was two orders of magnitude higher than the hydrogels (around 10 kPa). Incorporation of hydrogels resulted in increased equilibrium modulus of only GelMA, but not of other hydrogels. Presence of cells could result in loss of structural integrity of gels, and rapid degradation or dissolution of the gels due to matrix metalloproteinase (MMP) activity. The increase in modulus of GelMA (from 7 to 9 kPa) despite the decrease in its DW after 35 days of culture period (Fig. S2), could be due to high level of ECM production (Figs. 3 and 4). GelMA is prone to enzymatic degradation because it presents target sequences for MMPs [45]; however, the high ECM production on GelMA probably increased the compressive properties of this gel. Other researchers have also reported a decrease in the compressive modulus upon cell seeding [15,25]. Modulus of the hydrogels used in this study are similar to those obtained in other studies employing 2% agarose (10–15 kPa) [15,17], 10–15% GelMA (12–35 kPa) [17,24], and 2.5% HA (5–16 kPa) [23]. Although their equilibrium modulus could be increased to some extent by increasing the material concentration or crosslinking degree, these hydrogels still have considerably lower equilibrium modulus than that of the native meniscus (100–120 kPa) [46], making them unsuitable for use alone in meniscal replacement.

5. Conclusion

In this study, agarose, GelMA, MeHA, and GelMA-MeHA hydrogels, and 3D printed PCL were tested for *in vitro* meniscal regeneration. Hydrogels exhibited a higher production of ECM components than PCL. The level of cell-material interactions influenced the level and composition of the ECM produced on the hydrogels. GelMA, on which cells adhered strongly and assumed a dendritic morphology, exhibited a high level of collagen production. Agarose and MeHA, on which cells adhered weakly and assumed a round morphology, exhibited a high level of GAG production. Dynamic compression at up to 18% strain levels could be effective in enhancing ECM production, but higher strain levels could be catabolic for the cells. GelMA and agarose/MeHA could be used in regeneration of the inner and outer regions of the meniscus, respectively. The stiff 3D printed PCL could be combined with hydrogels to produce mechanically strong and functional scaffolds for meniscal regeneration.

Supplementary data to this article can be found online at https://doi.org/10.1016/j.ijbiomac.2018.09.065.

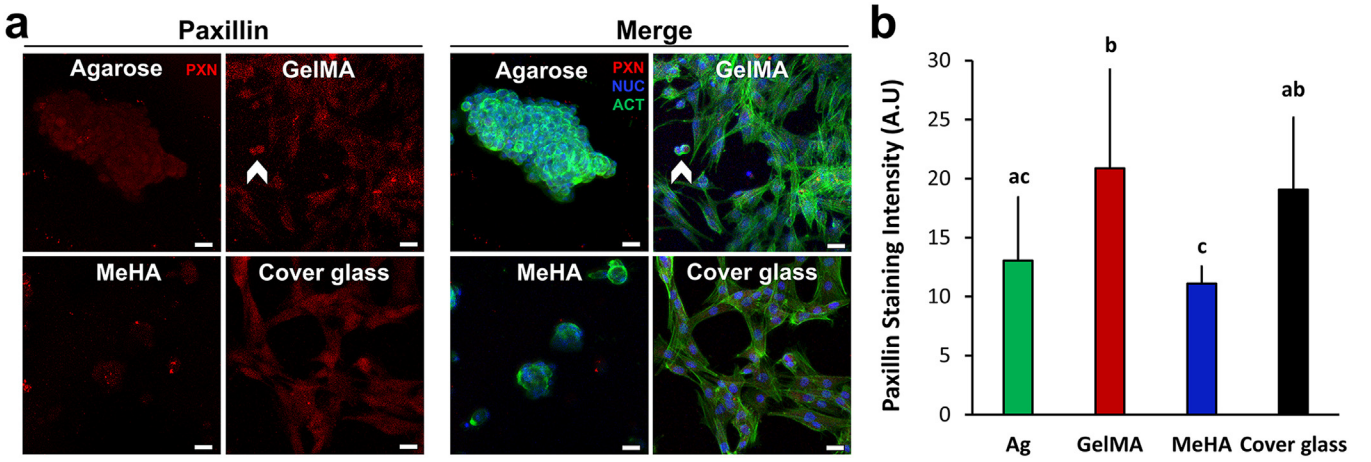

Fig. 6. The response of cells to the materials. (a) CLSM images of the gels stained for paxillin (PXN, red), nuclei (NUC, blue), and actin (ACT, green). Paxillin (left), and merge (right) images. Culture time: 21 days. Scale bars: 25 μm. Arrowheads point to the round cells. (b) Quantitative analysis showing paxillin staining intensities. [a, b, c, d, e]Significant difference between constructs when no letters in common.

Acknowledgements

This project was supported by BIOMATEN, METU [grant number BAP-08-11-2016-022]; the U.S. Department of Veterans Affairs Rehabilitation Research and Development Service [grant number 5IK2RX000760]. GB was supported by TUBITAK [through Bideb 2214/A]. BIOMATEN, the RIH Core Research Laboratories and Ginny Hovanesian are acknowledged for their contribution to histology and imaging.

Competing interests' statement

The authors declare that there is no conflict of interests.

Author contributions

GB: Collection and analysis of data, and preparation of manuscript.

GB, NH, BB, and VH: Study design, interpretation of data, and revision of manuscript.

BB and VH: provision of funding.

References

[1] J. Sanchez-Adams, V.P. Willard, K.A. Athanasiou, Regional variation in the mechanical role of knee meniscus glycosaminoglycans, J. Appl. Physiol. 111 (2011) 1590–1596.
[2] F.R. Noyes, S.D. Barber-Westin, Arthroscopic repair of meniscal tears extending into the avascular zone in patients younger than twenty years of age, Am. J. Sports Med. 30 (2002) 589–600.
[3] Y. Uchio, M. Ochi, N. Adachi, K. Kawasaki, J. Iwasa, Results of rasping of meniscal tears with and without anterior cruciate ligament injury as evaluated by second-look arthroscopy, Arthroscopy 19 (2003) 463–469.
[4] L.S. Lohmander, P.M. Englund, L.L. Dahl, E.M. Roos, The long-term consequence of anterior cruciate ligament and meniscus injuries: osteoarthritis, Am. J. Sports Med. 35 (2007) 1756–1769.
[5] J.E. Kuhn, E.M. Wojtys, Allograft meniscus transplantation, Clin. Sports Med. 15 (1996) 537–546.
[6] C. Van Der Straeten, P. Byttebier, A. Eeckhoudt, J. Victor, Meniscal allograft transplantation does not prevent or delay progression of knee osteoarthritis, PLoS ONE 11 (2016), e0156183.
[7] J. Banks, Adding value in additive manufacturing: researchers in the United Kingdom and Europe look to 3D printing for customization, IEEE Pulse 4 (2013) 22–26.
[8] C.H. Lee, S.A. Rodeo, L.A. Fortier, C. Lu, C. Erisken, J.J. Mao, Protein-releasing polymeric scaffolds induce fibrochondrocytic differentiation of endogenous cells for knee meniscus regeneration in sheep, Sci. Transl. Med. 6 (2014) 266ra171.
[9] E. Malikmammadov, T. Endogan, A. Kiziltay, V. Hasirci, N. Hasirci, PCL and PCL-based materials in biomedical applications, J. Biomater. Sci. Polym. Ed. 29 (2018) 863–893.
[10] T. Patrício, M. Domingos, A. Gloria, U. D'Amora, J.F. Coelho, P.J. Bártolo, Fabrication and characterisation of PCL and PCL/PLA scaffolds for tissue engineering, Rapid Prototyp. J. 20 (2014) 145–156.
[11] S. Buyuksungur, T. Endogan Tanir, A. Buyuksungur, E.I. Bektas, G. Torun Kose, D. Yucel, T. Beyzadeoglu, E. Cetinkaya, C. Yenigun, E. Tönük, V. Hasirci, N. Hasirci, 3D printed poly(ε-caprolactone) scaffolds modified with hydroxyapatite and poly(propylene fumarate) and their effects on the healing of rabbit femur defects, Biomater. Sci. 5 (2017) 2144–2158.
[12] A. Borzacchiello, A. Gloria, L. Mayol, Sally Dickinson, S. Miot, I. Martin, L. Ambrosio, Natural/synthetic porous scaffold designs and properties for fibro-cartilaginous tissue engineering, J. Bioact. Compat. Polym. 26 (2011) 437–451.
[13] N. Hasirci, C. Kilic, A. Komez, G. Bahcecioglu, H. Hasirci, Hydrogels in regenerative medicine, in: U. Demirci, A. Khademhosseini, M.R. Abidian, U.A. Gurkan (Eds.), Gels Handbook: Fundamentals, Properties and Applications Volume 2: Applications of Hydrogels in Regenerative Medicine, World Scientific Publishing, Singapore 2016, pp. 1–52.
[14] A. Rey-Rico, M. Cucchiarini, H. Madry, Hydrogels for precision meniscus tissue engineering: a comprehensive review, Connect. Tissue Res. 58 (2017) 317–328.
[15] C.T. Buckley, S.D. Thorpe, F.J. O'Brien, A.J. Robinson, D.J. Kelly, The effect of concentration, thermal history and cell seeding density on the initial mechanical properties of agarose hydrogels, J. Mech. Behav. Biomed. Mater. 2 (2009) 512–521.
[16] C.G. Wilson, J.F. Nishimuta, M.E. Levenston, Chondrocytes and meniscal fibrochondrocytes differentially process aggrecan during de novo extracellular matrix assembly, Tissue Eng. A 15 (2009) 1513–1522.
[17] A.C. Daly, S.E. Critchley, E.M. Rencsok, D.J. Kelly, A comparison of different bioinks for 3D bioprinting of fibrocartilage and hyaline cartilage, Biofabrication 8 (2016), 045002.
[18] G. Bahcecioglu, A. Buyuksungur, A. Kiziltay, N. Hasirci, V. Hasirci, Construction and in vitro testing of a multilayered, tissue-engineered meniscus, J. Bioact. Compat. Polym. 29 (2014) 235–253.
[19] J.J. Ballyns, L.J. Bonassar, Dynamic compressive loading of image-guided tissue engineered meniscal constructs, J. Biomech. 44 (2011) 509–516.
[20] M.C. McCorry, J.L. Puetzer, L.J. Bonassar, Characterization of mesenchymal stem cells and fibrochondrocytes in three-dimensional co-culture: analysis of cell shape, matrix production, and mechanical performance, Stem Cell Res Ther 7 (2016) 39.
[21] J.L. Puetzer, E. Koo, L.J. Bonassar, Induction of fiber alignment and mechanical anisotropy in tissue engineered menisci with mechanical anchoring, J. Biomech. 48 (2015) 1436–1443.
[22] K. Ishida, R. Kuroda, M. Miwa, Y. Tabata, A. Hokugo, T. Kawamoto, K. Sasaki, M. Doita, M. Kurosaka, The regenerative effects of platelet-rich plasma on meniscal cells in vitro and its in vivo application with biodegradable gelatin hydrogel, Tissue Eng. 13 (2007) 1103–1112.
[23] P.E. Donnelly, T. Chen, A. Finch, C. Brial, S.A. Maher, P.A. Torzilli, Photocrosslinked tyramine-substituted hyaluronate hydrogels with tunable mechanical properties improve immediate tissue-hydrogel interfacial strength in articular cartilage, J. Biomater. Sci. Polym. Ed. 28 (2017) 582–600.
[24] S.P. Grogan, P.H. Chung, P. Soman, P. Chen, M.K. Lotz, S. Chen, D.D. D'Lima, Digital micromirror device projection printing system for meniscus tissue engineering, Acta Biomater. 9 (2013) 7218–7226.
[25] P.A. Levett, D.W. Hutmacher, J. Malda, T.J. Klein, Hyaluronic acid enhances the mechanical properties of tissue-engineered cartilage constructs, PLoS ONE 9 (2014), e113216.
[26] G. Bahcecioglu, N. Hasirci, V. Hasirci, Effects of microarchitecture and mechanical properties of 3D microporous PLLA-PLGA scaffolds on fibrochondrocyte and L929 fibroblast behavior, Biomed. Mater. 13 (2018), 035005.
[27] J.W. Nichol, S.T. Koshy, H. Bae, C.M. Hwang, S. Yamanlar, A. Khademhosseini, Cell-laden microengineered gelatin methacrylate hydrogels, Biomaterials 31 (2010) 5536–5544.
[28] A. Komez, E.T. Baran, U. Erdem, N. Hasirci, V. Hasirci, Construction of a patterned hydrogel-fibrous mat bilayer structure to mimic choroid and Bruch's membrane layers of retina, J. Biomed. Mater. Res. A 104 (2016) 2166–2177.

[29] E. Hachet, H. Van Den Berghe, E. Bayma, M.R. Block, R. Auzély-Velty, Design of biomimetic cell-interactive substrates using hyaluronic acid hydrogels with tunable mechanical properties, Biomacromolecules 13 (2012) 1818–1827.
[30] G. Eke, N. Mangir, N. Hasirci, S. MacNeil, V. Hasirci, Development of a UV crosslinked biodegradable hydrogel containing adipose derived stem cells to promote vascularization for skin wounds and tissue engineering, Biomaterials 129 (2017) 188–198.
[31] C. Kilic Bektas, V. Hasirci, Mimicking corneal stroma using keratocyte loaded photopolymerizable methacrylated gelatin hydrogels, J. Tissue Eng. Regen. Med. 12 (2018) e1899–e1910.
[32] B. Bilgen, D. Chu, R. Stefani, R.K. Aaron, Design of a biaxial mechanical loading bioreactor for tissue engineering, J. Vis. Exp. 74 (2013), e50387.
[33] A.P. Hollander, T.F. Heathfield, C. Webber, Y. Iwata, R. Bourne, C. Rorabeck, A.R. Poole, Increased damage to type II collagen in osteoarthritic articular cartilage detected by a new immunoassay, J. Clin. Invest. 93 (1994) 1722–1732.
[34] Y. Liu, M.B. Chan-Park, A biomimetic hydrogel based on methacrylated dextran-graft-lysine and gelatin for 3D smooth muscle cell culture, Biomaterials 31 (2010) 1158–1170.
[35] J. Necas, L. Bartosikova, P. Brauner, J. Kolar, Hyaluronic acid (hyaluronan): a review, Vet. Med. 53 (2008) 397–411.
[36] A. Krouwels, F.P.W. Melchels, M.H.P. van Rijen, C.B.M. Ten Brink, W.J.A. Dhert, F. Cumhur Öner, M.A. Tryfonidou, L.B. Creemers, Focal adhesion signaling affects regeneration by human nucleus pulposus cells in collagen- but not carbohydrate-based hydrogels, Acta Biomater. 66 (2018) 238–247.
[37] S.P. Lake, V.H. Barocas, Mechanical and structural contribution of non-fibrillar matrix in uniaxial tension: a collagen-agarose co-gel model, Ann. Biomed. Eng. 39 (2011) 1891–1903.
[38] T.A. Ulrich, A. Jain, K. Tanner, J.L. MacKay, S. Kumar, Probing cellular mechanobiology in three-dimensional culture with collagen-agarose matrices, Biomaterials 31 (2010) 1875–1884.
[39] E. Schuh, S. Hofmann, K.S. Stok, H. Notbohm, R. Müller, N. Rotter, The influence of matrix elasticity on chondrocyte behavior in 3D, J. Tissue Eng. Regen. Med. 6 (2012) e31–e42.
[40] A. Karim, A.C. Hall, Chondrocyte morphology in stiff and soft agarose gels and the influence of fetal calf serum, J. Cell. Physiol. (5) (2016) 1041–1052.
[41] M. Freutel, A.M. Seitz, F. Galbusera, A. Bornstedt, V. Rasche, M.L. Knothe Tate, A. Ignatius, L. Dürselen, Medial meniscal displacement and strain in three dimensions under compressive loads: MR assessment, J. Magn. Reson. Imaging 40 (2014) 1181–1188.
[42] D.J. Huey, K.A. Athanasiou, Tension-compression loading with chemical stimulation results in additive increases to functional properties of anatomic meniscal constructs, PLoS ONE 6 (2011), e27857.
[43] M. Petri, K. Ufer, I. Toma, C. Becher, E. Liodakis, S. Brand, P. Haas, C. Liu, B. Richter, C. Haasper, G. von Lewinski, M. Jagodzinski, Effects of perfusion and cyclic compression on in vitro tissue engineered meniscus implants, Knee Surg. Sports Traumatol. Arthrosc. 20 (2012) 223–231.
[44] G. Du, H. Zhan, D. Ding, S. Wang, X. Wei, F. Wei, J. Zhang, B. Bilgen, A.M. Reginato, B.C. Fleming, J. Deng, L. Wei, Abnormal mechanical loading induces cartilage degeneration by accelerating meniscus hypertrophy and mineralization after ACL injuries in vivo, Am. J. Sports Med. 44 (2016) 652–663.
[45] T. Naqvi, T.T. Duong, G. Hashem, M. Shiga, Q. Zhang, S. Kapila, Relaxin's induction of metalloproteinases is associated with the loss of collagen and glycosaminoglycans in synovial joint fibrocartilaginous explants, Arthritis Res. Ther. 7 (2005) R1–11.
[46] A. Abdelgaied, M. Stanley, M. Galfe, H. Berry, E. Ingham, J. Fisher, Comparison of the biomechanical tensile and compressive properties of decellularised and natural porcine meniscus, J. Biomech. 48 (2015) 1389–1396.